Journal of Applied Genetics (2020) 61:477–488
https://doi.org/10.1007/s13353-020-00570-8

PLANT GENETICS • ORIGINAL PAPER

Cytological and genetic characterisation of dominant GMS line Shaan-GMS in *Brassica napus* L.

Xiaojuan Zhang[1,2,3] · Haiyan Chen[1,4,5] · Qian Zhang[1,4] · Yunxiao Zhang[1,4] · Zhaodi Xiao[1,4] · Yuan Guo[1,4] · Fei Yu[1,2] · Shengwu Hu[1,4]

Received: 11 December 2019 / Revised: 13 June 2020 / Accepted: 17 June 2020 / Published online: 26 July 2020

Abstract

Genic male sterility (GMS) is an effective pollination control system applied in the hybrid breeding of *Brassica napus* L. Shaan-GMS is a spontaneous mutant of dominant GMS in *B. napus*. In this research, anther abortion in the homozygous two-type line 9A15AB derived from Shaan-GMS was characterised with the combined use of light microscopy and transmission electron microscopy. Results indicated that the most striking differences between the fertile and sterile plants occurred in the tapetum in the early microsporocyte stage. In sterile plants, the tapetal cells were irregularly arranged, multi-layered and occupied the growing space of microsporocytes. When entering into meiosis, the tapetum cells degraded and the cytoplasm fused. Some oval monolayer or bilayer membrane organelles existed in the tapetal cells in sterile anthers. Mitochondria in the tapetal cells were abnormal, and middle layer cells degraded early. Pollen mother cells of Shaan-GMS degenerated at the start of meiosis and ceased at the anaphase I stage, with no dyads or tetrads formed. The combined effects of the abnormal development of the tapetum, the middle layer cells and meiosis lead to male sterility in Shaan-GMS. Inheritance of male sterility of Shaan-GMS is controlled by a monogenically multiallelic locus with three different alleles (*Ms*, *ms* and *Mf*), with a relationship expressed as *Mf* > *Ms* and *Ms* > *ms*. The findings help lay the foundation for illustrating the mechanism of male sterility and the utilisation of Shaan-GMS in rapeseed.

Keywords *Brassica napus* L. · Dominant genic male sterility · Meiosis · Microsporogenesis · Tapetum development

Introduction

Dominant genic male sterility (GMS) is a phenomenon wherein half of the plants in each generation are sterile when the sterile plants in this kind of GMS line are pollinated with fertile plants within the same species. However, further studies have indicated that in some cases when a male sterile genotype is crossed with a fertile genotype of the same species, the

Xiaojuan Zhang and Haiyan Chen contributed equally to this work.

Communicated by: Izabela Pawłowicz

Electronic supplementary material The online version of this article (https://doi.org/10.1007/s13353-020-00570-8) contains supplementary material, which is available to authorized users.

✉ Fei Yu
feiyu@nwsuaf.edu.cn

✉ Shengwu Hu
swhu83251@nwsuaf.edu.cn

[1] State Key Laboratory of Crop Stress Biology in Arid Areas, Northwest A&F University, Yangling 712100, Shaanxi, People's Republic of China

[2] College of Life Sciences, Northwest A&F University, Yangling 712100, Shaanxi, People's Republic of China

[3] School of Biological Science and Engineering, Shaanxi University of Technology, Hanzhong 723001, Shaanxi, People's Republic of China

[4] College of Agronomy, Northwest A&F University, Yangling 712100, Shaanxi, People's Republic of China

[5] College of Animal Science and Technology, Northwest A&F University, Yangling 712100, Shaanxi, People's Republic of China

F_1 generation is completely fertile, indicating that dominant male sterility can be restored (Kaul 1988; Liu 1991). This phenomenon has been observed in several important crops, including *Brassica napus* L. (Li et al. 1985, 1988), *B. rapa* (Zhang et al. 1990; Dong et al. 1998), rice (Yan et al. 1989) and millet (Hu et al. 1986). Two hypotheses have been suggested to explain this fertility restoration in the dominant male sterile plants. The first assumes that at least three multiple alleles, namely, *Mf*, *Ms* and *ms*, exist at the fertile locus. *Ms* is the male sterility allele, and *Mf* and *ms* are the fertility ones, with a relation *Mf* > *Ms* and *Ms* > *ms* (Ma et al. 1990; Feng et al. 1995; Song et al. 2005). The second hypothesis assumes that the male sterility in dominant GMS line is controlled by two pairs of dominant genes (*Ms* and *Rf*) in which *Ms* is the sterile gene and *Rf* is the restorer gene, and the *Ms* expression can be inhibited by *Rf*, leading to fertility restoration (Li et al. 1985, 1988; Zhou and Bai 1994). Both genetic models can explain the restoration phenomena of dominant GMS and can be used for rapeseed seed production by constructing a three-line hybrid system similar to cytoplasmic male sterility. To date, rapeseed hybrids based on this dominant GMS system have been successfully developed and approved in China (Zhou et al. 2006), indicating a promising future of this system in rapeseed hybrid breeding.

To date, several cases of rapeseed-dominant GMS accessions have been reported in China and overseas (Li et al. 1985; Mathias 1985; Dong and Du 1993; Hu et al. 1999; Wang et al. 2001; Wang et al. 2003; Song et al. 2005; Zeng et al. 2014). Of them, Yi3A and its derivatives have been regarded as representative of digenic interacting model by genetic studies (Li et al. 1985, 1988). However, recent allelism test results and molecular marker evidence suggest that 609AB and Rs1046AB derived from Yi3A are inherited as a multiple allele mode (Song et al. 2006a, b; Hong 2006; Liu et al. 2008).

In rapeseed, anther development can be divided into the following stages: sporangial cell, sporogenous cell, pollen mother cell, meiosis, mononuclear pollen, dinuclear pollen and trinuclear pollen stages. The anther wall layers consist of the epidermis, endothecium, middle layer and tapetum (Yu and Fu 1990). The tapetum, which is in the direct contact with the developing gametophytes in the anther locule, plays an important role in pollen development by supplying nutrients and lipid components and secreting mixtures of enzymes to disintegrate the callose wall surrounding the tetrads (Ariizumi and Toriyama 2011). The timely degradation of tapetum is crucial to the formation of pollen exine wall and occurs mainly after meiosis. The premature or delayed degradation of tapetal cells will lead to pollen abortion (Kawanabe et al. 2006; Parish and Li 2010; Luo et al. 2018). Several studies have been conducted on the cytological events of dominant male sterile anther development in rapeseed. Yu and Fu (1990) and Yang et al. (1999) showed that the anther abortion of Yi3A, a dominant GMS line in *B. napus*, occurs at the pollen mother cell (PMC) stage. The PMCs do not conduct meiosis, and no dyad or tetrad is formed. Wu and Yang (2008) revealed that male sterility of Rs1046AB, a dominant GMS *B. napus* line derived from Yi3A, is caused by meiotic abnormality and that no cells could pass the pachytene stage. Xin et al. (2016) further indicated that meiotic chromosomes of Rs1046A are arrested at the leptotene stage. Yan et al. (2016) revealed that the male gamete development of TE5A, a novel thermo-sensitive dominant GMS line in *B. napus*, is arrested at meiosis prophase I and that its homologous chromosomes could not pair, synapsis, and form bivalents. Xiao et al. (2013) conducted cytological observation on a dominant GMS line 0A30A derived from Shaan-GMS line in *B. napus* and observed several kinds of abnormal meiotic cells during the meiosis of sterile anthers. They concluded that PMCs of the dominant GMS line 0A30A are degenerated at the beginning of meiosis and could not pass the anaphase I stage, with no dyads or tetrads formed.

Shaan-GMS is a natural mutant of dominant GMS *B. napus* line discovered in 1994 (Hu et al. 1999). To date, homozygous two-type line, temporary maintainer line and restorer line have been developed and could be used to develop hybrid by the three-line system (Hu et al. 2002). However, its cellular mechanism of anther abortion and genetic model are still not well studied. The objectives of the present study were to (1) characterise the abortion period and subcellular events leading to anther abortion at microscopic and ultramicroscopic levels and (2) investigate the inheritance model of Shaan-GMS. The findings will provide insights into the mechanisms of anther abortion in Shaan-GMS and lay the foundation for its utilisation in rapeseed hybrid breeding.

Materials and methods

Plant materials

One homozygous two-type line (9A15AB), three temporary maintainer lines (9A01B, 9A08B and 9A09B) and two restorer lines (Zhong5R, Zhong7R) were used in the present study. The 9A15AB line was derived from the cross between one male sterile plant of Shaan-GMS and its restorer line (96-803), followed by consecutive sib-mating of the male sterile plants and fertile plants in progeny for more than 10 generations (Hu et al. 2002). In the homozygous two-type line 9A15AB, the sib-mating of sterile plants and fertile plants gave segregation in their progenies in a ratio 1:1 of sterile plants and fertile plants. All the rapeseed (*B. napus*) accessions were provided by the Rapeseed Research Centre of Northwest A&F University and planted in the experimental field of Northwest A&F University, Yangling, Shaanxi, during the crop seasons of 2009–2013.

Specimen processing for microscopy

The homozygous two-type line (9A15AB) was used for cytological observation. At the early flowering stage, the buds of different sizes from the main inflorescence were collected and immediately fixed in 4% glutaraldehyde in phosphate buffered saline (PBS 0.1 mol/L, pH 6.8) at 4 °C for 24 h. The specimens were washed with PBS (0.1 mol/L, pH 6.8) five times for 5, 10, 15, 20 and 30 min, respectively, at 4 °C and post-fixed in 1% osmium tetroxide in PBS (0.2 mol/L, pH 6.8) at 4 °C for 2 h. After washing with PBS for three times, the fixed anthers were dehydrated using a graded ethanol series. Then, the anthers were finally embedded in LR White resin (González-Melendi et al. 2008).

Light microscopy and transmission electron microscopy (TEM) analyses

Semi-thin sections (1 μm) were cut from the specimen block in a Leica EM UC7 ultramicrotome (Leica, Nussloch, Germany), stained with 1% toluidine blue solution, observed on a Leitz photomicroscope under bright field and photographed using an Olympus DC10 digital camera. For TEM analysis, ultrathin sections (70 nm) were obtained using a Reichert Ultracut S ultramicrotome, stained with a solution of 2% lead citrate and observed in a STEM LEO 910 electron microscope equipped and photographed with a Gatan Bioscan 792 digital camera.

Chromosome observation by 4′,6-diamidino-2-phenylindole (DAPI) staining and callose detecting by aniline blue staining

Inflorescences from sterile and fertile plants of 9A15AB were fixed in ethanol/acetic acid (3:1). One anther excised from a bud was squashed in a drop of acetocarmine solution by a dissecting needle on a glass slide and observed under a microscope to assess the meiotic stages. Then, the left anthers of the bud were stained with DAPI and viewed on a fluorescent microscope by using an UV filter (Ross et al. 1996). For callose staining, the left anthers from the bud were stained with 0.01% aniline blue and observed on a fluorescent microscope (Hong et al. 2001).

Genetic analysis

To determine whether the Shaan-GMS inheritance fits the multiple allele inheritance model or the digenic interacting model, we performed two types of tests. (1) The fertile plants (9A15B) of the homozygous two-type line 9A15AB were artificially emasculated and crossed with the temporary maintainers (9A01B, 9A08B). The fertile plants of the resulting F_1s were selfed and also test crossed with the temporary maintainers. This experiment will test whether the inhibition gene (or restorer gene, *Mf*) in the fertile plants is allelic to the *Ms* gene in the sterile plants from the homozygous two-type line based on the fertility performance of the selfing and test crossing progenies. (2) The sterile plants (9A15A) of the homozygous two-type line 9A15AB were crossed with the restorer lines (Zhong5R, Zhong7R), and the resulting F_1 plants were test crossed with the temporary maintainers (9A01B, 9A08B). The fertile plants in the test cross F_1s were selfed and back crossed with the temporary maintainers. This experiment aims to test whether the inhibition gene (*Mf*) in the restorer lines (Zhong5R, Zhong7R) is allelic to the *Ms* in the sterile plants from the homozygous two-type line. The fertility segregation ratio in each cross was investigated, and a Chi-square test was conducted in each cross if it had fertility segregation. Under the digenic interacting model, the male fertility was controlled by two pairs of genes, *Ms* and *ms* (*Ms* > *ms*) and *Mf* and *mf* (*Mf* > *mf*), with the dominance relationship of *Mf* > *Ms*. Under the multiple allele inheritance model, the male fertility was controlled by three alleles (*Mf*, *Ms*, *ms*) at one locus, with the dominance relationship of *Mf* > *Ms* > *ms* (Liu 1991; Song et al. 2006b). The hypothetical genotypes of sterile and fertile plants in the homozygous two-type line, temporary maintainers and restorer lines are indicated in Figs. S1 and S2.

Results

Morphological comparison of fertile and sterile plants in Shaan-GMS

No differences were observed between male fertile and sterile plants in the homozygous two-type line 9A15AB of Shaan-GMS before flowering. The difference between the two kinds of plants was observed in the floral organs during the flowering period. The flowers of fertile plants had long filaments, pollen loaded and yellow anthers, whereas the filaments of the flowers in sterile plants were shorter in length. The anthers were yellowish, small and dry, with no pollens (Fig. 1). Compared with the fertile plants, the initial flowering of the sterile plants was postponed for 3–4 days. Dead buds with white colour occasionally appeared in the sterile plants (as shown by white arrows in Fig. 1b).

Cytological observations of anther development in Shaan-GMS

During the sporogenous cell period, no apparent differences could be found between the male sterile and fertile anthers except that the PMCs in sterile anthers were vacuolated (Fig. S3a). At this stage, the four layers of the anther wall could be observed in male fertile (Fig. 2a) and sterile

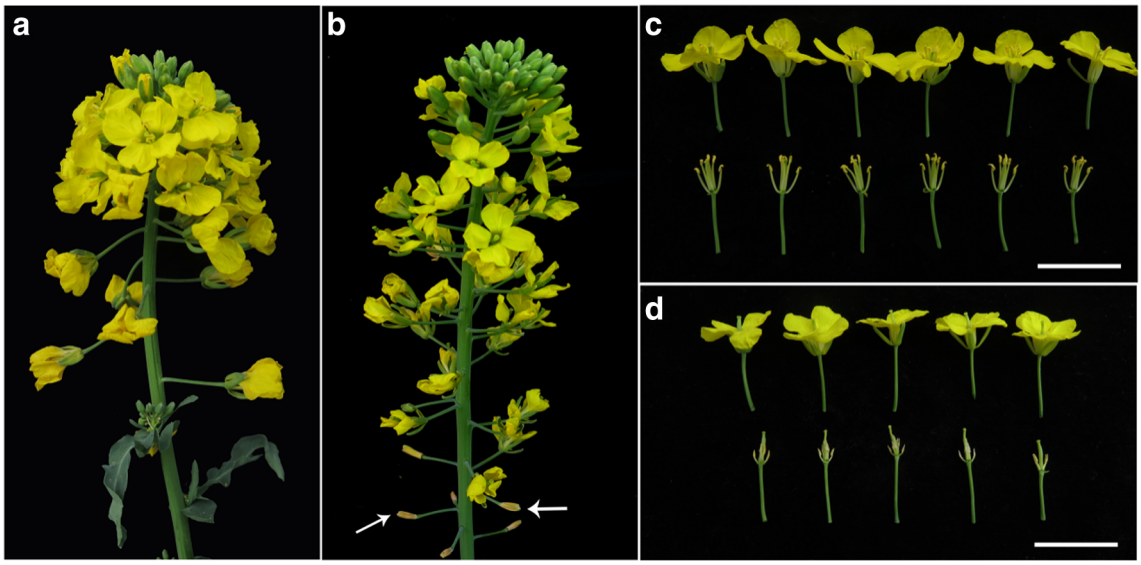

Fig. 1 Morphological comparison of floral organs between fertile (**a, c**) and male sterile (**b, d**) plants of Shaan-GMS. Scar bars = 2 cm (in **c** and **d**)

anthers (Fig. 2d). In the PMC stage, the PMCs gradually separated one from another (Figs. 2b, 2e). The earliest detectable abnormality in the male sterile anthers appeared in the tapetum cells at this stage. The tapetum cells of the sterile anthers were irregularly arranged, radially proliferated, multi-layered and squeezed out the growth space of the PMCs in some anther chambers (Fig. 2e). The multilayer tapetum cells degraded and the cytoplasm fused (Fig. S3b). When entering the meiosis stage, in fertile anthers, the PMCs were round, and the vacuoles in the tapetum cells shrunk (Fig. 2c). In sterile anthers, the middle layer cells disintegrated and stained light, and their cytoplasm was shrunk and vacuolated (Fig. S3c). The cytoplasm of the tapetum cells was also shrunk and disintegrated (Figs. 2f and S3d), and most PMCs stained grey and stopped development (Fig. S3d). In this process, however, a few of the PMCs in sterile anthers escaped cell autolysis and apoptosis and continued meiosis (Fig. 2f). In the tetrad stage, normal tetrads were observed in the anther sac in fertile plants (as shown by arrow; Fig. 2g), whereas in the sterile anthers, the cytoplasm of PMCs shrunk and disintegrated, and no tetrads were observed (Fig. 2j). In the uninucleate stage, in fertile anthers, young microspores were observed each with a nucleus in its centre (Fig. 2h). In sterile anthers, a few PMCs like 'pseudospores' were observed. The cytoplasm of these pseudospores gradually degraded, and the cytoplasm of the tapetum cells continued to degrade in sterile anthers (Fig. 2k). At the maturation stage, the mature pollen grains were formed in the pollen sac in fertile anthers, and the tapetum either completely disintegrated or some remnants maintained (Fig. 2i). Meanwhile, in sterile anthers, the pseudospores further disintegrated, leaving only a few dark stained substances in the pollen sac, and the tapetal cells were completely degraded (Fig. 2l).

Ultrastructure observation of anther development in Shaan-GMS

TEM analysis of the microspore development of sterile and fertile anthers in the homozygous two-type line 9A15AB of Shaan-GMS revealed that at the PMC stage, the cytoplasm of PMCs was thick and distributed a large number of organelles, including mitochondria, plastids and endoplasmic reticulum (ER) in fertile anthers (Fig. 3a). Meanwhile, in sterile anthers, the PMCs displayed plasmolysis, a large number of vacuoles were distributed in the cytoplasm, and the plastids were elongated (as shown by an arrow; Fig. 3e). When entering into the meiotic stage, various organelles were distributed in the cytoplasm of PMCs, and the nucleolus was nearly disappeared in fertile anthers (Fig. 3b), whereas in sterile anthers, in the cytoplasm of PMCs, the mitochondria became abnormally swelled, faint and fuzzy without cristae. The nucleus was apparently condensed with an obvious nucleolus and distributed many dark stained condensed chromatin (Fig. 3f). In some PMCs of sterile anthers, mitochondria and plastid bilayer membranes were ruptured, and electronically transparent regions were observed (Fig. S4a). In the uninucleate stage, mononuclear microspores were released from the tetrads in fertile anthers (Fig. 3c), whereas in sterile anthers, the cytoplasm of the 'pseudospores' contracted (Fig. 3g). In the mature stage, the mature pollen grains with intact exine were formed in fertile anthers (Fig. 3d), and the pseudospores in the sterile anther degraded into some kind of fibrous material (Fig. 3h).

The ultrastructure observation of the tapetum in sterile and fertile anthers indicated that at the PMC stage, the cytoplasm of tapetal cells in fertile anthers was thick had distributed mitochondria, plastids and other organelles; and had smaller and fewer vacuoles (Fig. 4a).

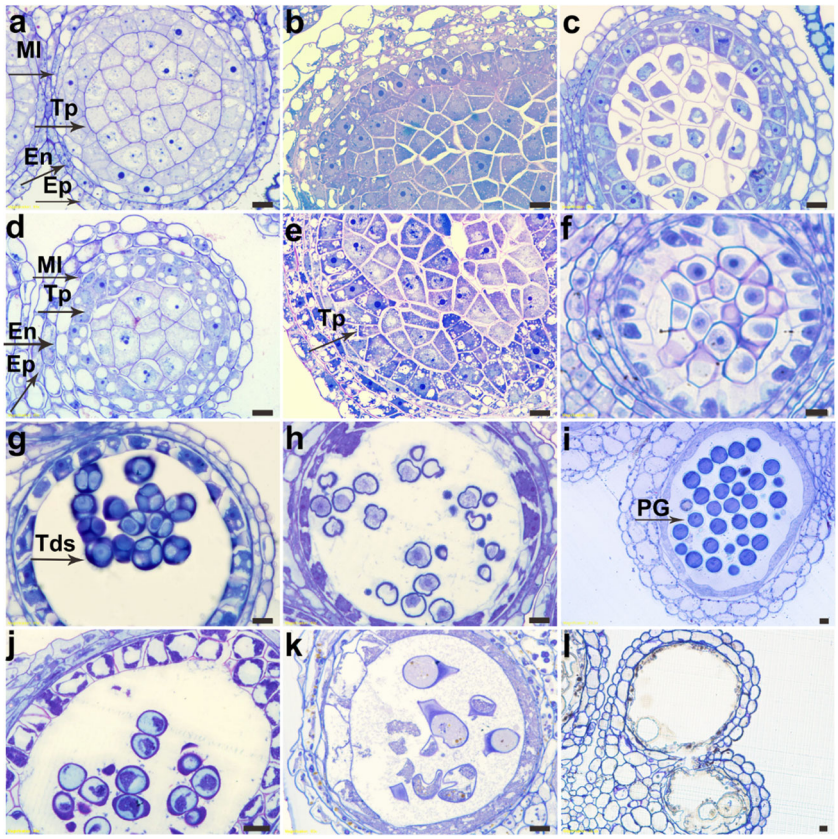

Fig. 2 Cytological observations of anther development in male fertile (**a**, **b**, **c**, **g**, **h**, **i**) and sterile (**d**, **e**, **f**, **j**, **k**, **l**) plants of Shaan-GMS. **a**, **d** Sporogenous cell stage. The four layers of the anther wall have been basically completed in this stage. No apparent differences could be found between the male sterile and fertile specimen. **b**, **e** Pollen mother cell stage. The pollen mother cells gradually separated. In sterile anthers (**e**), the tapetum cells were irregularly arranged, radially proliferated, multi-layered and squeezed out the growth space of the pollen mother cells in the anther chamber. **c**, **f** Meiosis period. In fertile anthers (**c**), the pollen mother cells became round; in sterile anthers (**f**), part of the pollen mother cells can enter into the late stage of meiosis I, and the tapetum cells showed plasmolysis. **g**, **j** Tetrad stage. The normal tetrads were formed in the anther sac in fertile plants (**g**); in sterile anthers (**j**), pollen mother cells like 'pseudospores' were formed in the anther chamber. **h**, **k** Uninucleate stage. In fertile anthers (**h**), the microspores were simply released from the tetrads, and the nucleus was at the centre of the cell; 'pseudospores' in sterile anther chamber (**k**) gradually degraded. Some tapetum cells degraded completely at this stage. **i**, **l** Mature stage. In fertile anthers (**i**), the mature pollen grains were formed in the pollen sac and the tapetum completely disintegrated, and some remnants could be observed. In the sterile anthers (l), 'pseudospores' further disintegrated, leaving only a few dark stained substances in the pollen sac, and the tapetal cells were completely degraded. Ep, epidermis; En, endothecium; MI, middle layer; Tp, tapetum; Tds, tetrads; PG, pollen grain. Scale bars = 10 μm

Meanwhile, in sterile anthers, mitochondria and other organelles became fuzzy, the nucleus was degraded, and the tapetal cells were severely vacuolised (Fig. 4e). When entering into the meiotic stage, in fertile plants, the tapetal cells contained abundant organelles, including mitochondria, plastids, ER and vacuoles, and the tapetal cell wall appeared wavy (Fig. 4b). In comparison, in sterile anthers, the middle layer cells had disintegrated cytoplasm and degraded cells (Fig. S4c). Moreover, the mitochondria in the cytoplasm of tapetal cells were abnormally expanded and became faint and fuzzy; the nucleus had an obvious nucleolus and distributed many dark stained condensed chromatin (Fig. 4f); and some elliptical monolayer or bilayer-coated organelles appeared (Fig. S4b). In the uninucleate stage, in the fertile plants, the tapetal cells contained a variety of organelles, including the elaioplasts, tapetosomes and ER (Fig. 4c). In sterile specimen, the cytoplasm of tapetal cells was shrunk and disintegrated (Fig. 4g). In the mature stage, in fertile anthers, the cell membrane of tapetal cells dissolved, and the contents were released into the locule to provide nutrients for the developing microspores (Fig. 4d). In sterile anthers, the tapetal cells were degraded, and only some residues were left in the anther sac (Fig. 4h).

Chromosomal behaviour of PMCs in Shaan-GMS

At the leptotene stage, in fertile PMCs, several bright-stained chromatin centres were visible, and the chromosome displayed a beaded-like structure (Fig. 5a). Compared with the fertile specimen, the chromosomes of sterile PMCs were located on one side of the nucleus (Fig. 5d). At the pachytene stage, the chromosomes become short and thick in both fertile and sterile PMCs (Fig.

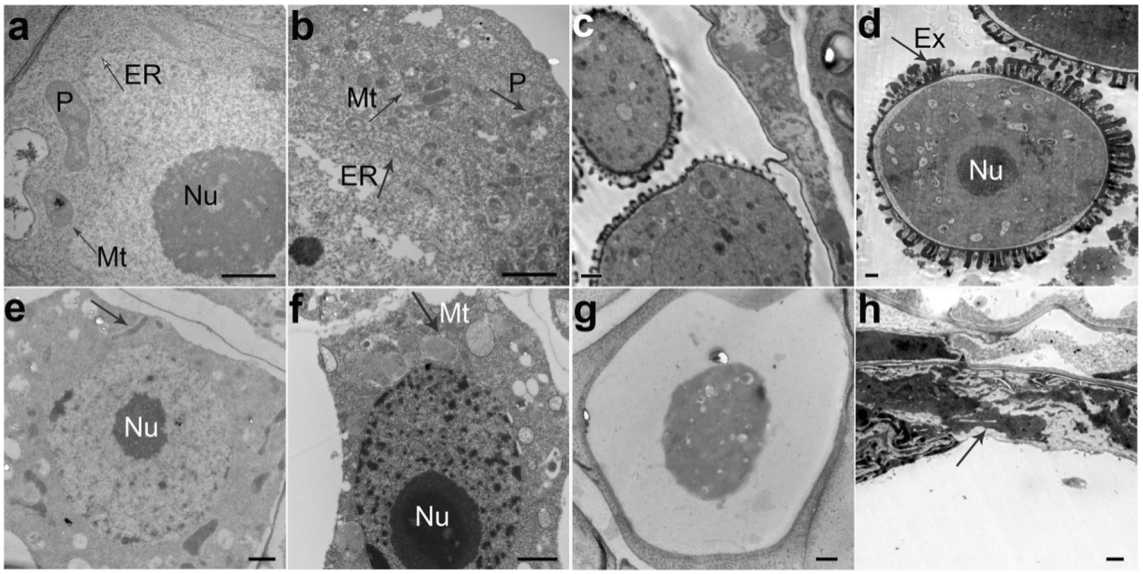

Fig. 3 Transmission electron micrographs of microspore development in fertile (**a**, **b**, **c**, **d**) and male sterile (**e**, **f**, **g**, **h**) anthers of Shaan-GMS. **a**, **e** Pollen mother cell stage. In fertile anthers, the cytoplasm of pollen mother cells (PMCs) was thick and distributed a large number of organelles, including mitochondria, plastids and endoplasmic reticulum (**a**); in sterile anthers, the PMCs displayed plasmolysis and plastids are elongated (as shown by arrow), and a large number of vacuoles were distributed in the cytoplasm (**e**). **b**, **f** Meiotic stage. In fertile anthers, the cytoplasm of PMCs distributed various organelles (**b**); in the cytoplasm of PMCs in sterile anthers, mitochondria were abnormally expanded, faint and fuzzy without cristae in them; the nucleus was apparently condensed and degraded (**f**). **c**, **g** Uninucleate stage. Mononuclear microspores just released from the tetrads in fertile anthers (**c**); in sterile anther sac, the cytoplasm of the 'pseudospores' contracted (**g**). **d**, **h** Mature stage. The mature pollen grains with intact exine were formed in fertile anthers (**d**); 'pseudospores' in the sterile anther sac degraded into some fibrous materials (**h**). ER, endoplasmic reticulum; Mt, mitochondrion; P, plastid; Nu, nucleus; Ex, exine. Scale bars = 1 μm

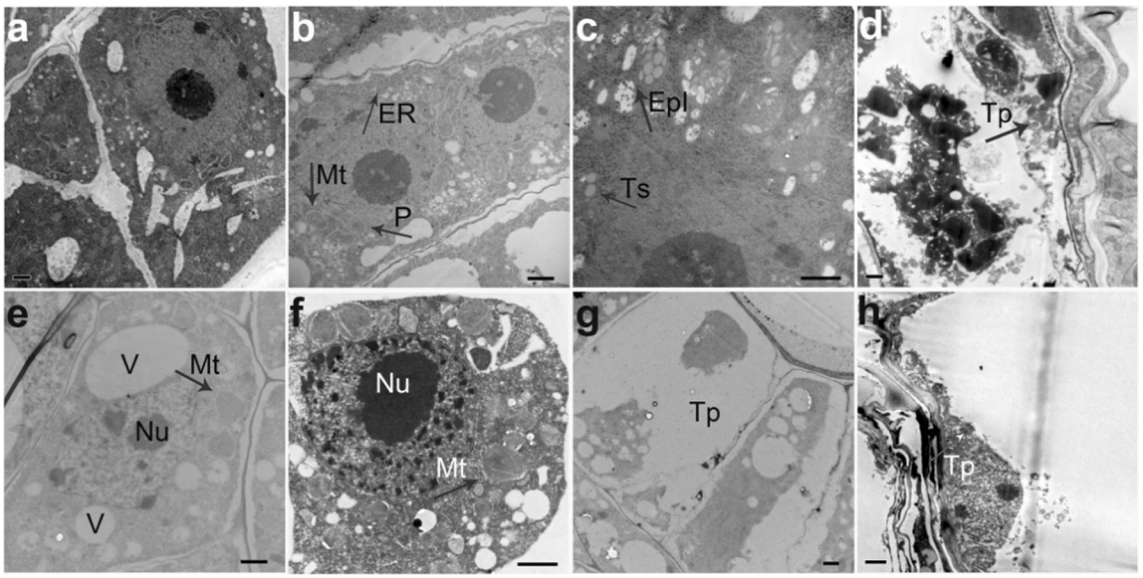

Fig. 4 Transmission electron micrographs of tapetum development in fertile (**a**, **b**, **c**, **d**) and male sterile (**e**, **f**, **g**, **h**) anthers of Shaan-GMS. **a**, **e** Pollen mother cell stage. In fertile plants, the cytoplasm of tapetal cells was thick and distributed mitochondria, plastids and other organelles, and the vacuoles were small and few (**a**); in sterile plants, mitochondria and other organelles became fuzzy, the nucleus degraded, and the tapetal cells were severely vacuolised (**e**). **b**, **f** Meiotic stage. In fertile plants (**b**), the tapetum cells contained two nuclei and abundant organelles, including the mitochondria, plastids, endoplasmic reticulum and vacuoles. The tapetal cell wall appeared wavy; in the cytoplasm of tapetum cells of sterile plants (**f**), mitochondria were abnormally expanded and became faint and fuzzy, and the nucleus was condensed and degraded. **c**, **g** Uninucleate stage. In fertile plants, the tapetum became mature that contained a variety of organelles, including the elaioplasts, tapetosomes and endoplasmic reticulum (**c**); in sterile specimen, the cytoplasm of tapetum cells was shrunk, and the tapetum cells were degraded (**g**). **d**, **h** Mature stage. In fertile plants, the cell membrane of tapetum cells dissolved, and the contents were released into the locule (**d**); in sterile specimen, the tapetum cells were degraded, and only some residues were left in the anther sac (**h**). ER, endoplasmic reticulum; Mt, mitochondrion; P, plastid; Nu, nucleus; V, vacuoles; Tp, tapetum; Epi, elaioplast; Ts, tapetosome. Scale bars = 1 μm

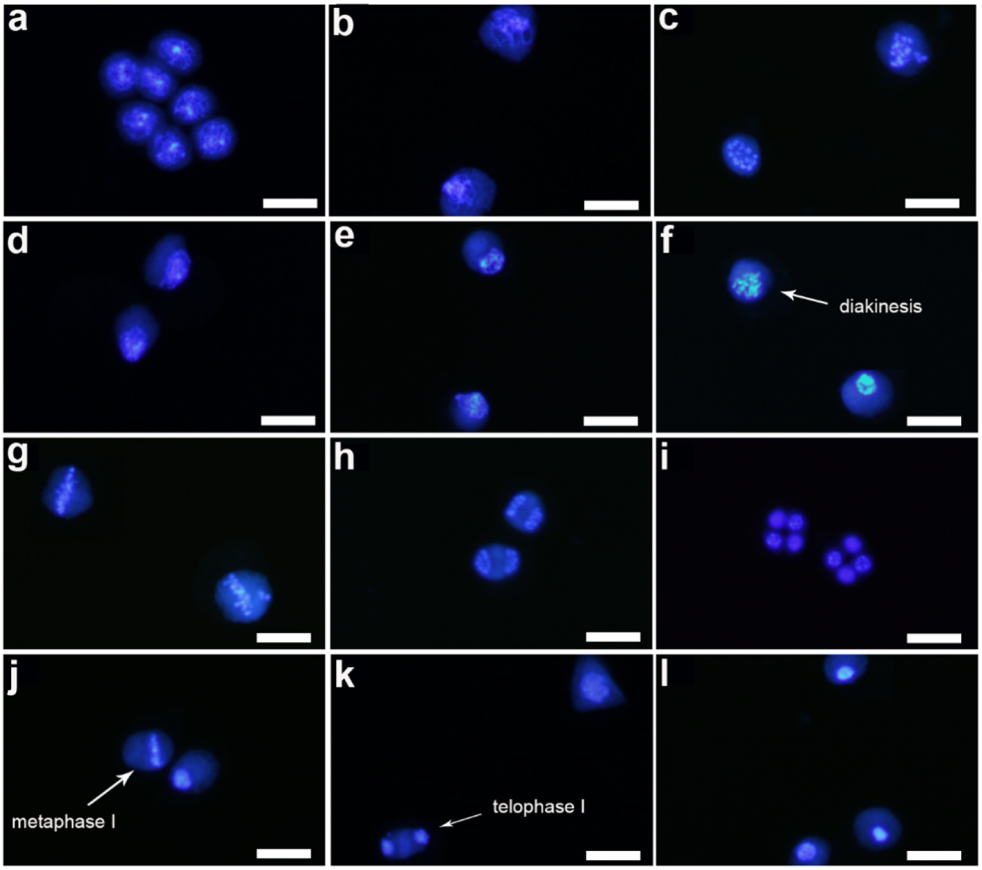

Fig. 5 Meiosis in fertile (**a**, **b**, **c**, **g**, **h**, **i**) and sterile (**d**, **e**, **f**, **j**, **k**, **l**) plants of Shaan-GMS by using the spreading technique stained with DAPI. **a**, **d** Leptotene. Compared with the fertile specimen (**a**), the chromosomes of sterile specimen were located on the side of the nucleus (**d**). **b**, **e** Pachytene. **c**, **f** Diakinesis. **g**, **j** Metaphase I. **h**, **k** Telophase I. Compared with the fertile specimen (**c**, **g**, **h**), meiosis was unsynchronised, and only a few of pollen mother cells could undergo this process in sterile specimen (**f**, **j**, **k**). **i**, **l** Telophase II. In fertile specimen, normal tetrads were formed (**i**). However, in sterile specimen, no tetrads were formed, and the nuclei of pollen mother cells or 'pseudospores' were condensed (**l**). Scale bars = 20 μm

5b, e). In fertile anthers, the PMCs can pass through the meiosis stage and enter into the tetrad stage (Fig. 5 c, g, h and i). In sterile specimens, only a few of the PMCs can pass through the diakinesis and metaphase I and stayed at telophase I (Fig. 5 f, j and k). No tetrads were formed, and the nuclei of PMCs condensed at the stage corresponding to the tetrad stage in fertile specimen (Fig. 5l). Aberrant features, such as rod-shaped chromosomes (Fig. S5a), double nuclei (Fig. S5b), three nuclei (Fig. S5c) and micronuclei (Fig. S5d), can also be observed in PMCs in sterile specimen by DAPI staining.

Callose staining of PMCs in Shaan-GMS

At the pre-meiosis and meiosis stages, callose signals can be detected in both male fertile (Fig. 6a, b) and sterile PMCs (Fig. 6d, e). At the early microspore stage, no signals can be detected in fertile specimens (Fig. 6c), whereas signals can be detected in sterile specimen (Fig. 6f), indicating that callose on the 'pseudospores' surfaces was not degraded.

Genetic analysis of the Shaan-GMS

As shown in Table 1, all F_1s between the fertile plants (9A15B) of the homozygous two-type line 9A15AB and the temporary maintainers (9A01B, 9A08B) indicated fertility segregation at a ratio of 1:1 of sterile and fertile plants. The progeny was all fertile both in selfing of fertile plants in F_1 generation and in back cross between F_1 and temporary maintainers. According to the fertility performance of progenies under the two genetic models (Fig. S1), the restorer gene *Mf* in the fertile plants (9A15B) was allelic to the male sterile gene *Ms* in the male sterile plants in the homozygous two-type line 9A15AB.

The F_1 generations from crosses between sterile plants (9A15A) of the homozygous two-type line 9A15AB and the two restorer lines (Zhong5R, Zhong7R) were all fertile. The test crosses between F_1s and the temporary maintainers segregated in the 1:1 ratio of sterile and fertile plants. Then, the fertile plants from the above test crosses were both selfed and test crossed with the temporary maintainers. The progenies of selfing and test crosses were all fertile (Table 2). These results indicated that the restorer gene *Mf* in the restorer lines was allelic to the sterile gene *Ms* in sterile plants in the homozygous two-type line 9A15AB (Fig. S2).

Based on the above results, the inheritance of Shaan-GMS fits the genetic model of one multiple allele locus with three different alleles (*Ms*/*ms*/*Mf*). Here, *Ms* is the mutant sterile gene, *ms* is the wild-type fertile gene, and *Mf* is the restorer gene, with a dominant relationship of *Mf* > *Ms* > *ms*.

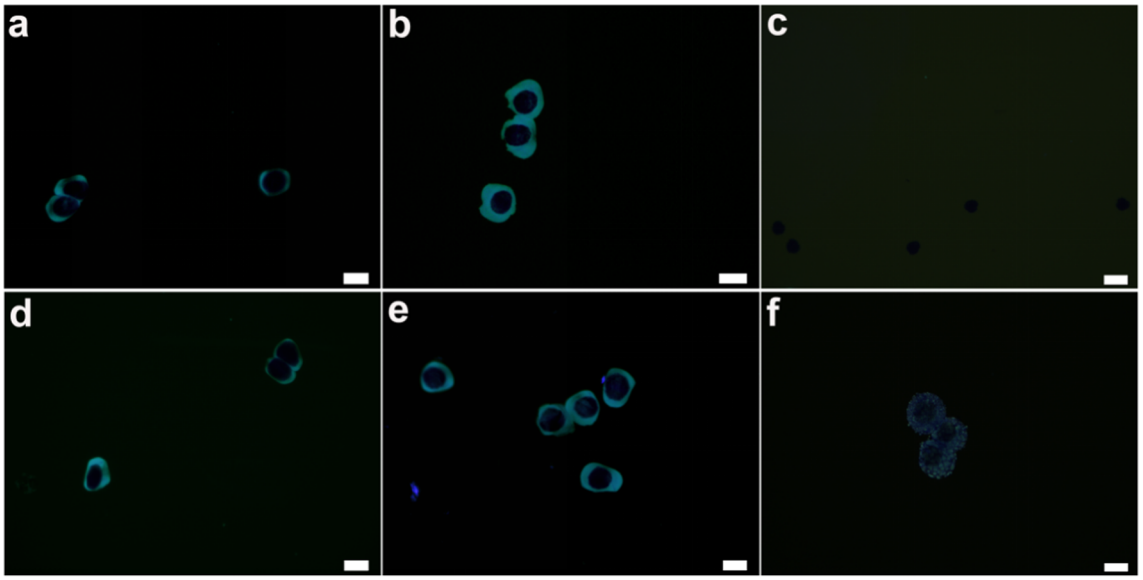

Fig. 6 Callose observation in fertile (**a**, **b**, **c**) and male sterile (**d**, **e**, **f**) pollen mother cells in Shaan-GMS during meiosis stained with aniline blue. **a**, **d** Pre-meiosis stage. **b**, **e** Meiosis stage. **c**, **f** Early microspore stage. No signals can be detected in fertile specimen (**c**), whereas in sterile specimen (**f**), some stained substances on the 'pseudospores' surface could be observed. Scale bars = 20 μm

Discussion

Aberrant cytological characters during anther development in Shaan-GMS

Several studies have been conducted on cytological events of dominant GMS in rapeseed. Yu and Fu (1990) and Yang et al. (1999) indicated that anther abortion of the dominant GMS line Yi3A in *B. napus* occurred at the PMC stage. The PMCs did not conduct meiosis, and no dyad or tetrad was formed. Wu and Yang (2008) and Xin et al. (2016) revealed that the meiosis of the dominant GMS line Rs1046AB derived from Yi3A ceased at the pachytene or leptotene stage, finally leading to its pollen abortion. The male gamete development of the thermo-sensitive dominant GMS line TE5A in *B. napus* was arrested at meiosis prophase I (Li et al. 2016; Yan et al. 2016). Xiao et al. (2013) reported that the PMCs of the dominant GMS line 0A30A, which was derived from Shaan-GMS in *B. napus*, degenerated at the beginning of meiosis and could not pass the anaphase I stage, with no dyads or tetrads formed. In the present study, by the combined use of light microscopy and TEM, we observed various abnormalities of anther development in Shaan-GMS, including nuclei-condensed PMCs, cells with micronuclei, collapsed cells, plasmolysis cells and microspore analogue developed from PMCs without meiosis but enclosed by the exine wall. This result is consistent with

Table 1 The fertility performance of the test cross between the fertile plants in homozygous two-type line and the temporary maintainers

Year	Field no.	Hybrid combination	Fertile plants	Sterile plants	Fertile/sterile (χ^2) (1:1)
2011	0A55	9A15B × 9A01B (maintainer-1)	87	89	0.005
	0A57	9A15B × 9A08B (maintainer-2)	55	57	0.009
2012	1A45	0A55-3B × 0A01-3B (maintainer-1)	98	0	
	1A46	0A55-4B × 0A01-4B (maintainer-1)	93	0	
	1A47	0A57-1B × 0A08-1B (maintainer-2)	88	0	
	1A48	0A57-2B × 0A08-2B (maintainer-2)	71	0	
	1A49	0A55-3B⊗	30	0	
	1A50	0A55-4B⊗	32	0	
	1A51	0A57-1B⊗	33	0	
	1A52	0A57-2B⊗	35	0	

χ^2 (0.05, 1) = 3.84

Table 2 The fertility performance of the test cross between the sterile plants in homozygous two-type line and the temporary maintainers

Year	Filed no.	Hybrid combinations	Fertile plants	Sterile plants	Fertile/Sterile(χ^2) (1:1)
2011	0A39	9A15A × 9A49 (Zhong5R)	80	0	
	0A49	9A15A× 9C390 (Zhong7R)	80	0	
2012	1A34	0A39-1B × 0A01-1B (maintainer-1)	133	119	0.67
	1A35	0A39-1B × 0A09-1B (maintainer-2)	181	158	1.43
	1A41	0A49-1B × 0A09-1B	109	97	0.59
	1A43	0A49-1B × 0A01-1B	56	43	1.45
2013	2A01	1A34-1B × 1A01-1B(maintainer-1)	208	0	
	2A07	1A34-2B × 1A09-1B(maintainer-2)	210	0	
	2A08	1A34-3B × 1A09-1B	211	0	
	2A17	1A35-1B × 1A01-1B	187	0	
	2A19	1A35-2B × 1A01-1B	213	0	
	2A20	1A35-3B × 1A09-1B	214	0	
	2A28	1A41-1B × 1A09-1B	69	0	
	2A30	1A41-2B × 1A01-1B	35	0	
	2A31	1A43-1B × 1A09-1B	157	0	
	2A35	1A34-1B⊗	105	0	
	2A36	1A34-2B⊗	97	0	
	2A37	1A34-3B⊗	114	0	
	2A38	1A35-1B⊗	120	0	
	2A39	1A35-2B⊗	80	0	
	2A40	1A35-3B⊗	93	0	
	2A41	1A41-1B⊗	95	0	
	2A42	1A41-2B⊗	145	0	
	2A44	1A43-1B⊗	199	0	

χ^2 (0.05, 1) = 3.84

that reported by Xiao et al. (2013). Furthermore, we observed some novel cytological phenomena about pollen abortion in Shaan-GMS. For instance, we found mitochondria abnormality in the tapetal cells at the early stage of meiosis. The middle layer cells of the male sterile anthers in Shaan-GMS were extruded and prematurely disintegrated. Some elliptical monolayer or bilayer-coated organelles were also found in the tapetum cells at the end of meiosis—a condition that may affect the normal PCD of the tapetum. DAPI staining revealed that meiosis of Shaan-GMS stopped at the telophase I stage. All these aberrant cytological events finally resulted in the male sterility of Shaan-GMS.

In the flowering plants, tapetum development plays an important role in anther development; premature or delayed degeneration of the tapetum leads to pollen abortion (Kawanabe et al. 2006; Li et al. 2006; Vizcay-Barrena and Wilson 2006). In the present study, various abnormalities of tapetum development were observed in Shaan-GMS. For instance, the structure of the tapetum cells changed, showing an irregular and multi-layer arrangement. Furthermore, normal PCD was affected in tapetum cells in Shaan-GMS. In the early stage of meiosis, distinct features of PCD, such as chromatin aggregates and cytoplasmic shrinkage and disintegration, can be found in the tapetum cells. In the PMC stage, the vacuolated tapetal cells can also be found in the Shaan-GMS. Moreover, at the end of the meiosis stage, some elliptical monolayer or bilayer-coated organelles appeared in the tapetum cells. In *Ogu* CMS of *B. napus*, tapetal cells with enlarged ER which encloses parallel striations were observed at premeiotic stages of microsporogenesis (Polowick and Sawhney 1990). In Ogu-IRNA CMS of *B. napus*, pale, oval or round-shaped organelles with a double membrane and inner membraneous structures were observed in the tapetal cells during tetrad to vacuolate microspore stages (González-Melendi et al. 2008). So we deduced that the elliptical monolayer or bilayer-coated organelles in the tapetum cells observed in the present study may be derived from ER.

Compared with the studies on tapetum function, few studies have explored the role of the middle layer cells in anther development (Kawanabe et al. 2006; Li et al. 2006; Falasca et al. 2013). In this study, at the early stage of meiosis, we observed that the middle layer cells of the male sterile anthers in Shaan-GMS were extruded and prematurely disintegrated by the hypertrophic multi-layer tapetum. In plants, the pollen exine is

usually the largest Ca^{2+} reservoir (Tian et al. 1998). In gymnosperms and some dicotyledons, it has been reported that Ca^{2+} is transported to the tapetum from the middle layer and secreted from the tapetum to the anther chamber (Kong and Jia 2004; Chen et al. 2008; Qiu et al. 2009; Falasca et al. 2013). Falasca et al. (2013) indicated that in the male sterile anthers of the kiwi fruit, the degradation of the tapetum and the middle layer is delayed. This delay may prolong the secretion of the pollen outer wall components, such as sporopollenin and Ca^{2+} in the tapetum and the middle layer, resulting in microspore development abnormality. In Arabidopsis, the middle layer cells degrade earlier than the tapetum. However, in a tapetum-expanded mutant, the middle layer cells do not degrade and perform a function similar to the tapetum (Sanders et al. 1999). The *MALE STERILITY1* (*MS1*) gene is important for the development of tapetum and the formation of pollen walls (Yang et al. 2007). The PCD event displayed in the *ms1* middle layer almost extends to dehiscence, and the middle layer does not degrade earlier than the wild type (Vizcay-Barrena and Wilson 2006). In rice, tapetum degeneration requires a basic helix-loop-helix transcription factor encoding gene—the *tapetum degeneration retardation* (*tdr*) gene. However, in *tdr* mutants, the degeneration of the tapetum and the middle layer was delayed, leading to microspore collapse (Li et al. 2006). Thus, we deduced that the premature disintegration of the middle layer cells may be related to anther abortion in rapeseed Shaan-GMS.

Considering the abortion time of anther development and various abnormalities in Shaan-GMS, we suggested that Shaan-GMS differs from the other dominant GMS lines reported so far in rapeseed.

Genetic analysis of Shaan-GMS

Dominant GMS is of particular significance in crop breeding because of its usefulness in population improvement by recurrent selection and hybrid seed production. To date, some dominant GMS lines have been reported in *B. napus*, and restorer lines have been found for several dominant GMS lines as well, including Yi3A and its derivatives (Li et al. 1985), 2626A (Dong and Du 1993), Qianyou 2AB (Wang et al. 2001), Shaan-GMS (Hu et al. 2004), and 609AB (Song et al. 2005). Two genetic models, namely, digenic interacting model and one multiple allele model, have been suggested to explain the fertility recovery of dominant GMS. Li et al. (1985, 1988) proposed that dominant GMS was controlled by two pairs of dominant genes in dominant GMS line 23A derived from Yi3A. Liu (1991) proposed the ABC genetic test to distinguish the two genetic models. Recently, genetic analysis and molecular marker evidence suggested that dominant GMS lines 609AB and Rs1046AB derived from Yi3A inherit as a multiple allele mode (Song et al. 2006a, b; Hong 2006; Liu et al. 2008). The triallelic genetic male-sterile locus (*BnMs5*) in the dominant GMS line Rs1046AB (609AB) was mapped on the *B. napus* A8 chromosome (Lu et al. 2013), and *MS5* encodes a *Brassica*-specific protein carrying conserved coiled-coil and DUF626 domains with unknown function (Xin et al. 2016), and molecular mechanisms underpinning the multiallelic inheritance of *MS5* were recently revealed (Xin et al. 2020). The $MS5^d$ gene, which is responsible for male sterility in *B. napus* thermo-sensitive dominant GMS line TE5E, was also mapped on the *B. napus* A8 chromosome (Zeng et al. 2014); $MS5^d$ and $MS5^b$ share a common ancestor *MS5* and are derived from neofunctionalization of its ancestor by different mechanisms; $MS5^b$ contains an 8815-bp *Mutator*-like transposable element (MULE) in the second intron that differs when compared with $MS5^a$ (Xin et al. 2016); whereas $MS5^d$ contains a C-1524-T transition, encoding a Leu-281-Phe substitution (Zeng et al. 2017). In *B. rapa,* the three-allele model was also reported for two sources of dominant GMS lines (Feng et al. 2009; Lin et al. 2020). Both the *Ms* gene in *B. rapa* ssp. *pekinensis* (Feng et al. 2009) and *BrMs* gene in *B. rapa* ssp. *chinensis* (Lin et al. 2020) are mapped on the *B. rapa* A07 chromosome, but they differ from each other. Interestingly, *BrMs* from *B. rapa* is allelic to *BnRf* in 9012A (Xie et al. 2012; Deng et al. 2016; Lin et al. 2020), a different kind of GMS line in *B. napus,* which male sterility was regarded to be conferred by *BnMs3*/*Bnms3* and the *BnRf* locus including three alleles (Dong et al. 2012; Dun et al. 2014). In the present research, we used the back cross and test cross strategy with temporary maintainer and revealed that the inheritance of dominant GMS line Shaan-GMS was controlled by a multiple allele model with three different alleles (Liu 1991; Song et al. 2006b), thereby indicating the relationship given by *Mf* > *Ms* > *ms*. Our previous test cross results showed that Shaan-GMS has a similar maintaining and restoring relationship with 6CA derived from Yi3A in *B. napus* (Hu et al. 2004), and our recent results showed that the fertility genes of Shaan-GMS were also mapped to the *B. napus* A08 chromosome (not published). Whether those cases of *B. napus* dominant GMS are controlled by the same locus needs to be further investigated. The findings can help lay the foundation for the use of Shaan-GMS in rapeseed hybrid breeding in the future.

Authors' contributions SH conceived and designed research. XZ, HC, QZ, YZ and ZD performed the experiments. SH and XZ analysed the data and wrote the manuscript. YG and FU participated in the review of the manuscript. All the authors read and approved the final manuscript.

Funding information This study was funded by the Key Research and Development Project in Shaanxi Province of China (2018ZDXM-NY-008), the Modern Crop Seed Industry Project of Shaanxi Province (20171010000004) and the Qinling-Bashan Mountains Bioresources Comprehensive Development C.I.C. (QBXT-17-5).

Compliance with ethical standards

Conflict of interest The authors declare that they have no conflict of interest.

Ethical approval This article does not contain any studies with human participants or animals performed by any of the authors.

References

Ariizumi T, Toriyama K (2011) Genetic regulation of sporopollenin synthesis and pollen exine development. Annu Rev Plant Biol 62:437–460

Chen SH, Liao JP, Luo MZ, Kirchoff BK (2008) Calcium distribution and function during anther development of *Torenia fournieri* (Linderniaceae). Ann Bot Fenn 45:195–203

Deng ZH, Li X, Wang ZZ, Jiang YF, Wan LL, Dong FM, Chen FX, Hong DF, Yang GS (2016) Map-based cloning reveals the complex organization of the *BnRf* locus and leads to the identification of *BnRf* ^{b}, a male sterility gene, in *Brassica napus*. Theor Appl Genet 129: 53–64

Dong YL, Du H (1993) Study on a dominant genetic male sterility discovered in *Brassica napus* L. Southwest China J Agric Sci 04:6–10

Dong ZS, Liu CS, Jing JS, Zhuang SQ, Ran LG (1998) Selection and breeding of double dominant nuclear sterility of 896AB in *B. campestrics* L. Acta Agron Sin 24(2):187–192

Dong F, Hong D, Xie Y, Wen Y, Dong L, Liu P, He Q, Yang G (2012) Molecular validation of a multiple-allele recessive genic male sterility locus (*BnRf*) in *Brassica napus* L. Mol Breed 30:1193–1205

Dun X, Shen W, Hu K, Zhou Z, Xia S, Wen J, Yi B, Shen J, Ma C, Tu J, Fu T, Lagercrantz U (2014) Neofunctionalization of duplicated *Tic40* genes caused a gain-of-function variation related to male fertility in *Brassica oleracea* lineages. Plant Physiol 166:1403–1419

Falasca G, Angeli SD, Biasi R, Fattorini L, Matteucci M, Canini A, Altamura MM (2013) Tapetum and middle layer control male fertility in *Actinidia deliciosa*. Ann Bot Lond 112:1045–1055

Feng H, Wei YT, Xu M (1995) Genetic models for genic male sterile line of Chinese cabbage and its verification. Essays on Horticulture, The second annual youth academic conference of the Chinese Association for Science and Technology. Beijing Agricultural University Press, Beijing, pp 458–466

Feng H, Wei P, Piao ZY, Liu ZY, Li CY, Wang YG, Ji RQ, Ji SJ, Zou T, Choi SR, Lim YP (2009) SSR and SCAR mapping of a multiple-allele male-sterile gene in Chinese cabbage (*Brassica rapa* L.). Theor Appl Genet 111:333–339

González-Melendi P, Uyttewaal M, Morcillo CN, Mora JRH, Fajardo S, Budar F, Lucas MM (2008) A light and electron microscopy analysis of the events leading to male sterility in Ogu-INRA CMS of rapeseed (*Brassica napus*). J Exp Bot 59(4):827–838

Hong DF (2006) Mapping of the *Ms*/*Mf* gene of a dominant genic male sterility in *Brassica napus* L. Dissertation, Huazhong Agriculture University

Hong Z, Delauney AJ, Verma DPS (2001) A cell-plate specific callose synthase and its interaction with phragmoplastin. Plant Cell 13:755–768

Hu HK, Ma SY, Shi YH (1986) The discovery of a dominant male sterile gene in millet (*Setaria italica*). Acta Agron Sin 12(2):73–78

Hu SW, Yu CY, Zhao HX, Ke GL (1999) The genetic of a new kind of male sterility accession "Shaan-GMS" in *Brassica napus* L. Acta Bot Boreal-Occident Sin 19(6):63–67

Hu SW, Yu CY, Zhao HX, Lu M (2002) Development of GMS homozygous two-type line 803AB from dominant GMS Shaan-GMS in *Brassica napus* L. Acta Agric Boreali-occidentalis Sin 11(4):25–27

Hu SW, Yu CY, Zhao HX, Lu M, Zhang CH, Yu YJ (2004) Identification and genetic analysis of the fertility restoring gene for dominant male sterility accession "Shaan-GMS" in *Brassica napus* L. J Northwest Sci Tech Univ Agric For (Natural Sci Ed) 32(4):9–12

Kaul MLH (1988) Male sterility in higher plants. Springer Verlag, Berlin and Heidelberg

Kawanabe T, Ariizumi T, Kawai-Yamada M, Uchimiya H, Toriyama K (2006) Abolition of the tapetum suicide program ruins microsporogenesis. Plant Cell Physiol 47:784–787

Kong HY, Jia GX (2004) Calcium distribution during pollen development of *Larix principis-rupprechtii*. Acta Bot Sin 46:69–76

Li SL, Qian YX, Wu ZH (1985) Inheritance of genic male sterility in *Brassica napus* and its application to commercial production. Acta Agric Shanghai 1(2):1–12

Li SL, Qian YX, Wu ZH, Stefansson BR (1988) Genetic male sterility in rape (*Brassica napus* L.) conditioned by interaction of genes at two loci. Can J Plant Sci 68:1115–1118

Li N, Zhang DS, Liu HS, Yin CS, Li XX, Liang WQ, Yuan Z, Xu B, Chu HW, Wang J, Wen TQ, Huang H, Luo D, Ma H, Zhang DB (2006) The rice tapetum degeneration retardation gene is required for tapetum degradation and anther development. Plant Cell 18(11):2999–3014

Li KQ, Zeng XH, Yuan R, Yan XH, Wu G (2016) Cytological researches on the anther development of a thermo-sensitive genic male sterile line TE5A in *Brassica napus*. Sci Agric Sin 49(12):2408–2417

Lin ZT, Lin YP, Lin SF (2020) Genetic analysis and fine mapping of a spontaneously mutated male sterility gene in *Brassica rapa* ssp. *chinensis*. G3-Genes Genomes Genet 10:1309–1318

Liu DF (1991) The theoretical studies on the restoration for genic male sterility in plants. J Hubei Agric Col 11:1–9

Liu J, Hong DF, Lu W, Liu PW, He QB, Yang GS (2008) Genetic analysis and molecular mapping of gene associated with dominant genic male sterility in rapeseed (*Brassica napus* L.). Genes Genom 30(2):523–532

Lu W, Liu J, Xin Q, Wan L, Hong D, Yang G (2013) A triallelic genetic male sterility locus in *Brassica napus*: an integrative strategy for its physical mapping and possible local chromosome evolution around it. Ann Bot 111:305–315

Luo CC, Sun YY, Zhang YX, Guo Y, Klima M (2018) Genetic investigation and cytological comparison of two genic male sterile lines 9012A and MSL in *Brassica napus* L. Euphytica 214(7):124

Ma SY, Dong QF, Chen HJ (1990) A preliminary report on the discovery of the multiple alleles in millet which dominate male sterility. Hereditas 12(1):9–11

Mathias R (1985) A new dominant gene of male sterility in rapeseed (*Brassica napus* L.). Z Pflanzenzuchtung 94(2):170–173

Parish RW, Li SF (2010) Death of a tapetum: a programme of developmental altruism. Plant Sci 178:73–89

Polowick PL, Sawhney VK (1990) Microsporogenesis in a normal line and in the *ogu* cytoplasmic male-sterile line of *Brassica napus* I. The influence of high temperatures. Sex Plant Reprod 3:263–276

Qiu YL, Liu RS, Wei DM, Tian HQ (2009) Calcium distribution in developing anthers of lettuce (*Lactuca sativa*). Ann Bot Fenn 46: 101–106

Ross KJ, Fransz P, Jones GH (1996) A light microscopic atlas of meiosis in *Arabidopsis thaliana*. Chromosom Res 4(7):507–516

Sanders PM, Bui AQ, Weterings K, McIntire KN, Hsu YC, Lee PY, Truong MT, Beals TP, Goldberg TB (1999) Anther developmental defects in *Arabidopsis thaliana* male-sterile mutants. Sex Plant Reprod 11:297–322

Song LQ, Fu TD, Yang GS, Tu JX, Ma CZ (2005) Genetic verification of multiple allelic gene for dominant genic male sterility in 609AB (*Brassica napus* L.). Acta Agron Sin 31(7):869–875

Song LQ, Fu TD, Tu JX, Ma CZ, Yang GS (2006a) Molecular validation of multiple allele inheritance for dominant genic male sterility gene in *Brassica napus* L. Theor Appl Genet 113(1):55–62

Song LQ, Fu TD, Yang GS, Tu JX, Ma CZ (2006b) Allelism analysis of dominant genic male sterility gene and its restorer gene in *Brassica napus*. Sci Agric Sin 39(03):456–462

Tian HQ, Kuang A, Musgrave ME, Russell SD (1998) Calcium distribution in fertile and sterile anthers of a photoperiod-sensitive genic male-sterile rice. Planta 204:183–192

Vizcay-Barrena G, Wilson ZA (2006) Altered tapetal PCD and pollen wall development in the Arabidopsis ms1 mutant. J Exp Bot 57: 2709–2717

Wang TQ, Huang ZS, Tian ZP, Dai WD (2001) The sterility identification and genetics analysis of newly bred GMS line Qianyou 2AB in *B. napus*. Southwest China J Agric Sci 14(1):46–49

Wang DJ, Tian JH, Wang H, Hu XP, Li DR, Guo AG (2003) RAPD markers linked to mono-dominant GMS in rapeseed. Acta Bot Boreal-Occident Sin 23(9):1556–1560

Wu JY, Yang GS (2008) Meiotic abnormality in dominant genic male sterile *Brassica napus*. Mol Biol 42(4):645–651

Xiao ZD, Xin XY, Chen HY, Hu SW (2013) Cytological investigation of anther development in DGMS line Shaan-GMS in *Brassica napus* L. Czech J Genet Plant Breed 49(1):16–23

Xie YZ, Dong FM, Hong DF, Wan LL, Liu PW, Yang GS (2012) Exploiting comparative mapping among *Brassica* species to accelerate the physical delimitation of a genic male-sterile locus (*BnRf*) in *Brassica napus*. Theor Appl Genet 125:211–222

Xin Q, Shen Y, Li X, Lu W, Wang X, Han X, Dong FM, Wan LL, Yang GS, Hong DF, Cheng ZK (2016) *MS5* mediates early meiotic progression and its natural variants may have applications for hybrid production in *Brassica napus*. Plant Cell 28:1263–1278

Xin Q, Wang X, Gao YP, Xu DD, Xie ZQ, Dong FM, Wan LL, Yang LY, Yang GS, Hong DF (2020) Molecular mechanisms underpinning the multiallelic inheritance of *MS5* in *Brassica napus*. Plant J. https://doi.org/10.1111/tpj.14857

Yan LA, Zhang JC, Zhu C, Ou YH, Li JN, Cai YH (1989) The preliminary evaluation of a dominant male sterile gene in rice. Acta Agron Sin 15(2):174–181

Yan XH, Zeng XH, Wang SS, Li KQ, Yuan R, Gao HF, Luo JL, Liu F, Wu YH, Li YJ, Zhu L, Wu G (2016) Aberrant meiotic prophase I leads to genic male sterility in the novel TE5A mutant of *Brassica napus*. Sci Rep-Uk 6:33955. https://doi.org/10.1038/srep33955

Yang GS, Qu B, Fu TD (1999) Anatomical observations on the anther's development of the dominant genic male sterile line Yi-3A in *Brassica napus* L. J Huazhong Agric Univ 18(5):405–408

Yang C, Vizcay-Barrena G, Conner K, Wilson ZA (2007) MALE STERILITY1 is required for tapetal development and pollen wall biosynthesis. Plant Cell 19:3530–3548

Yu FQ, Fu TD (1990) Cytomorphological research on anther development of several male-sterile lines in *Brassica napus* L. J Wuhan Bot Res 8(3):209–216

Zeng XH, Li WP, Wu YH, Liu F, Luo JL, Gao YL, Zhu L, Li YJ, Li J, You QB, Wu G (2014) Fine mapping of a dominant thermosensitive genic male sterility gene (*BntsMs*) in rapeseed (*Brassica napus*) with AFLP- and *Brassica rapa*-derived PCR markers. Theor Appl Genet 127:1733–1740

Zeng XH, Yan XH, Yuan R, Li KQ, Wu YH, Liu F, Luo JL, Li J, Wu G (2017) Identification and analysis of $MS5^{d}$: A gene that affects double-strand break (DSB) repair during meiosis I in *Brassica napus* microsporocytes. Front Plant Sci 7:1966

Zhang SF, Song ZH, Zhao XY (1990) Breeding of interactive genic male sterile line in Chinese cabbage (*Brassica pekinensis* Rupr) and utilization model. Acta Hortic Sin 17(2):117–125 (in Chinese)

Zhou YM, Bai HH (1994) Identification and genetic studies of the inhibition of dominant male sterility in *Brassica napus*. Plant Breed 113: 222–226

Zhou XR, Zhuang J, Sun CC, Li SL, Sai XF, Hu GB, Wang WR, Li YL, Gu LD, Qian XF (2006) Breeding of a dominant genic male sterility (GMS) hybrid variety Heza 7 of *Brassica napus* L. with double low (erucic acid and glucosinolate) content in rapeseed. Acta Agric Shanghai 22(4):6–9